r-Shaped Hybrid Nanogenerator with Enhanced Piezoelectricity

Mengdi Han,[†,§] Xiao-Sheng Zhang,[†,§] Bo Meng,[†] Wen Liu,[†,‡] Wei Tang,[†] Xuming Sun,[†] Wei Wang,[†] and Haixia Zhang[†,*]

[†]National Key Lab of Nano/Micro Fabrication Technology, Peking University, Beijing, China and [‡]Peking University Shenzhen Graduate School, Shenzhen, China. [§]These authors contributed equally to this work.

ABSTRACT Piezoelectric and triboelectric nanogenerators (NGs) have been proposed in the past few years to effectively harvest mechanical energy from the environment. Here, a polydimethylsiloxane (PDMS) layer is placed under the aluminum electrode of polyvinylidene fluoride (PVDF), thus forming an r-shaped hybrid NG. Micro/nanostructures have been fabricated on the PDMS surface and the aluminum electrodes of PVDF to enhance the output performance. Power densities of the piezoelectric part and the triboelectric part are 10.95 and 2.04 mW/cm^3, respectively. Moreover, influence of the triboelectric charges on the piezoelectric output voltage is investigated. Both finite element method simulations and experimental measurements are conducted to verify this phenomenon. The novel hybrid NG is also demonstrated as a power source for consumer electronics. Through one cycle of electric generation, 10 light-emitting diodes are lighted up instantaneously, and a 4-bit liquid crystal display can display continuously for more than 15 s. Besides, the device is integrated into a keyboard to harvest energy in the typing process.

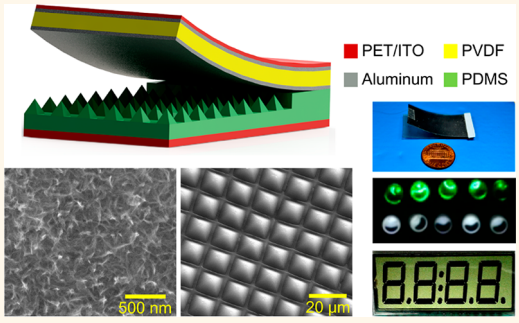

KEYWORDS: piezoelectric nanogenerator · triboelectric nanogenerator · enhanced piezoelectricity · self-powered system

As is well-known, energy crises are becoming a worldwide problem, and researchers are making every effort to search for the green and renewable energy source. To solve the problem, self-powered systems have been proposed, which focus on harvesting energy from the ambient environment using different transduction mechanisms.[1−4] Among various kinds of energy in the environment, mechanical energy is relatively stable and widely distributed. Vibration energy harvesters based on different working principles (*i.e.*, electromagnetic,[5] electrostatic,[6] piezoelectric[7]) have been developed and studied. With the advantage of high output voltage, piezoelectric harvesters have drawn a lot of attention. Piezoelectric nanogenerators (NGs) using ZnO,[8] polyvinylidene fluoride (PVDF),[9] PZT,[10] $BaTiO_3$,[11] *etc.* have been measured and show good output performance. Moreover, new piezoelectric materials such as t-Te[12] and PMN-PT nanowires[13] have also been utilized recently in piezoelectric NGs.

For one kind of piezoelectric NG, the piezoelectric layer is bent and recovered to generate voltage, in which case the electrode will inevitably have friction with the substrate material. The friction can be utilized to generate energy based on the combination of triboelectric and electrostatic effect.[14,15] For triboelectric NGs, the electric charge is produced due to the different triboelectric polarity between two materials. Then, as the value of the equivalent capacitance changes, electrons will flow in the external circuit. Based on different triboelectric NG structures, change of capacitor can be achieved by varying the gap distance[16,17] and contact area.[18,19] Through alteration of the structure, triboelectric NGs can be applied to biomedical[20] and environmental[21,22] systems as a power supply or a self-powered active sensor. Combined with triboelectric NGs, solar cells[23] and electrochemical cells[24] have been fabricated and have obtained good results, too.

In this work, we present an r-shaped hybrid NG to generate electricity through mechanical input. The piezoelectric NG and the triboelectric NG are combined together to enhance the output performance. Given an external force, both piezoelectric

* Address correspondence to zhang-alice@pku.edu.cn.

Received for review May 20, 2013 and accepted September 13, 2013.

Published online September 13, 2013
10.1021/nn404023v

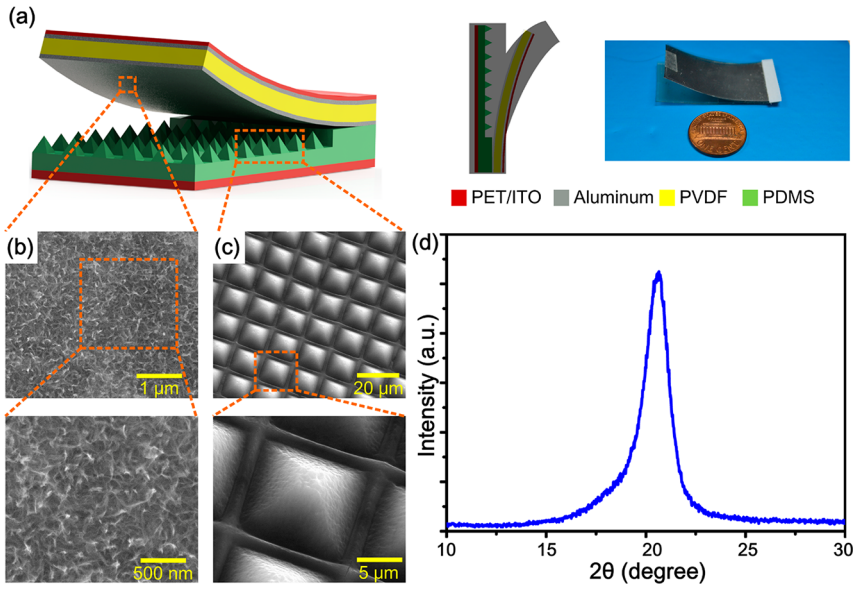

Figure 1. (a) Schematic view and photograph of the hybrid NG. (b) SEM images of the nanostructured aluminum electrode. (c) SEM images of the MNDS PDMS. (d) XRD analysis of the polarized PVDF.

and triboelectric output can be generated. Micro/nanostructures have been fabricated on the surface to further enhance the output. Besides, the triboelectric charges will affect the piezoelectric output by enhancing or reducing the piezoelectric potential.

RESULTS AND DISCUSSION

Working Principle. Figure 1a shows the schematic diagram and photograph of the fabricated r-shaped hybrid NG. The upper part (*i.e.*, the piezoelectric NG) consists of a 100 μm polarized PVDF film, surface-nanostructured Al electrodes, and a PET film. The PET film is bent to be arc-shape, with an arc length of 4 cm and diameter of 6.5 cm. The lower part (*i.e.*, the triboelectric NG) is made up by the micro/nano dual-scale (MNDS) polydimethylsiloxane (PDMS),[25] PET/ITO electrode, and the bottom surface-nanostructured Al electrode. The two parts are fixed at one end, forming an r-shaped structure. Moreover, the friction surfaces are both micro/nanostructured to increase the surface roughness[26] for enhanced triboelectric output.[20,27] Through hot deionized water treatment,[28] nanostructures can be clearly observed on the Al surface, as shown in Figure 1b. Replication from the silicon mold fabricates MNDS PDMS as shown in Figure 1c. X-ray diffraction (XRD) analysis of the polarized PVDF is shown in Figure 1d. The 20° peak indicates the dominant β-phase in the PVDF, which is crucial for the piezoelectric effect.

Under mechanical forces, the r-shaped hybrid NG can generate piezoelectric as well as triboelectric output depending on the external connection. In the original state, no charges exist on the surface of the Al electrode and PDMS. After a few cycles of movement, negative charges are accumulated on the PDMS surface, while positive charges exist on the bottom Al electrode. Then, given an external force (Figure 2a), the upper surface of PVDF will experience a tensile stress, while the compressive stress is yielded at the lower surface. In this case, the PVDF generates a d_{31} mode piezoelectric potential, which will produce a charge flow if the two Al electrodes are connected (dashed line). Meanwhile, gap distance between PDMS and the bottom Al electrode decreases. This will produce a triboelectric output if the ITO electrode and bottom Al electrode are connected (solid line). Soon afterward, the hybrid NG is pressed and charges reach equilibrium (Figure 2b). Both piezoelectric and triboelectric output reduce to zero at this state. When the external force is canceled (Figure 2c), the PVDF tends to recover to its original shape. The stress direction changes at the surface of PVDF, thus generating a reversed piezoelectric potential. Besides, the gap between PDMS and the bottom Al electrode increases, which changes the

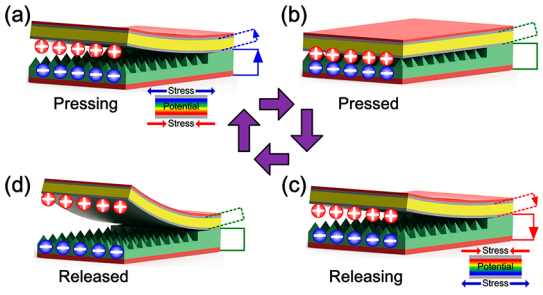

Figure 2. Working principle of the hybrid NG. (a) Pressing state. PVDF is bent and gap distance decreases, producing forward piezoelectric and triboelectric output. (b) Pressed state. Charges reach equilibrium and produce no electrical output. (c) Releasing state. PVDF is recovered and gap distance increases, producing reversed piezoelectric and triboelectric output. (d) Released state. Charges reach equilibrium and produce no electrical output.

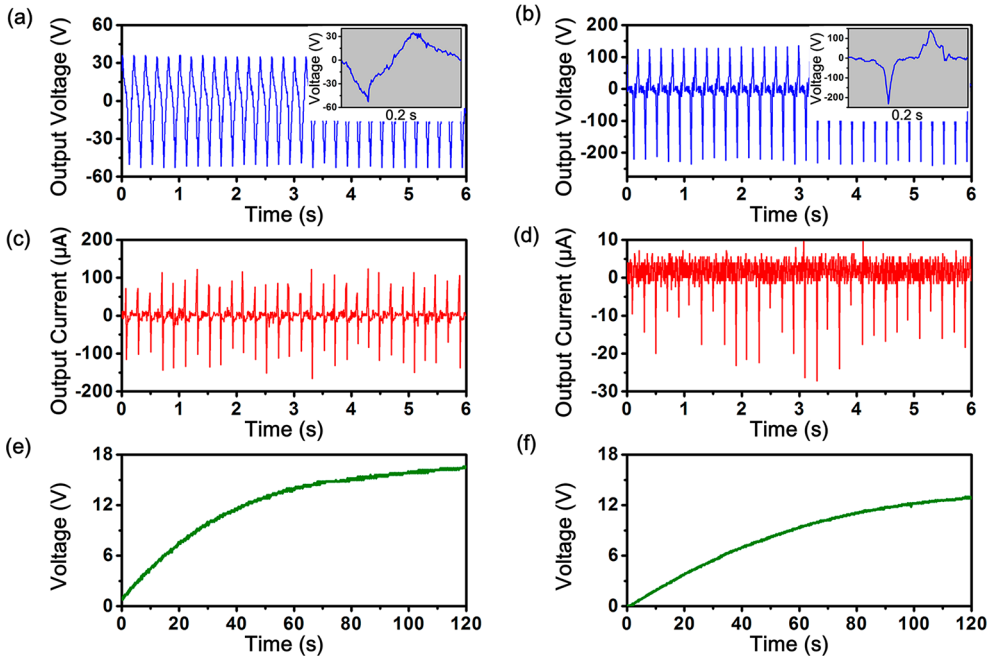

Figure 3. Output characterization. (a) Output voltage of the piezoelectric NG. The inset shows an enlarged voltage curve in one cycle. (b) Output voltage of the triboelectric NG. The inset shows an enlarged voltage curve in one cycle. (c) Output current of the piezoelectric NG. (d) Output current of the triboelectric NG. (e) Voltage of a 1 μF capacitor charged by the piezoelectric NG. (f) Voltage of a 1 μF capacitor charged by the triboelectric NG.

electric field between the friction materials. With proper external connections, the piezoelectric potential and the changed electric field will drive the charges in the external circuit to flow in an opposite direction. Finally, the hybrid NG is released and reaches equilibrium again, thus achieving a movement cycle (Figure 2d).

Output Characterization. Output performance of the hybrid NG is investigated using a vibration system. First, output voltage of the hybrid NG is measured with a 100 MΩ probe at the frequency of 5 Hz. Given an external force, the PVDF bends to generate voltage. As shown in Figure 3a, the peak voltage reaches up to 52.8 V with a 35.1 ms half-wave width. For the triboelectric part, the output peak voltage is 4.5 times higher (240 V, shown in Figure 3b), due to the micro/nanostructured friction surfaces. Since the micro/nanostructures increase the surface roughness, the friction will be more thorough and more triboelectric charges will be generated.[29] (Detailed discussion is shown in Figure S1 in the Supporting Information.) However, the half-wave width of the peak generated by the triboelectric part is only 8 ms, which is much smaller than that of the piezoelectric part. For the output current, both the piezoelectric part and the triboelectric part are measured using a 10 kΩ external resistance. As shown in Figure 3c,d, the output currents of the piezoelectric part and the triboelectric part are 166 and 27.2 μA, respectively.

Through comparison, the piezoelectric NG has a smaller output voltage but larger output current, which is caused by the relatively low equivalent resistance. In detail, the equivalent resistance of a piezoelectric NG can be expressed as[30]

$$R_p = \frac{d}{A\varepsilon_p f} \quad (1)$$

where d, A, and ε_p are the thickness, area, and permittivity of the piezoelectric material (*i.e.*, PVDF) and f is the frequency of the external force. As for the triboelectric NG, the expression of its equivalent resistance is more complex. Based on the capacitor model, the calculated equivalent resistance is determined by the permittivity of the dielectric (*i.e.*, PDMS), size of the device, and frequency of the external force. Moreover, unlike the piezoelectric NG, the movement equation of the top electrode under the external force will also influence the equivalent resistance. (Detailed calculation is shown in Figure S2 in the Supporting Information.) To compare the equivalent resistance of the piezoelectric NG and the triboelectric NG, output voltages of the series-connected NGs and parallel-connected NGs are measured. When the two NGs are in series connection, the output peak voltage reaches 328 V and the voltage signal is similar to the triboelectric output. For the parallel connection, the output voltage is like the piezoelectric output with a peak value of 58.6 V. By analyzing the equivalent circuit, it can be concluded from the results that the equivalent resistance of the triboelectric NG is larger than that of the piezoelectric NG (discussed in Figure S3 in the Supporting Information).

Considering the power output, instantaneous power density as high as 1.10 mW/cm^2 is achieved for the

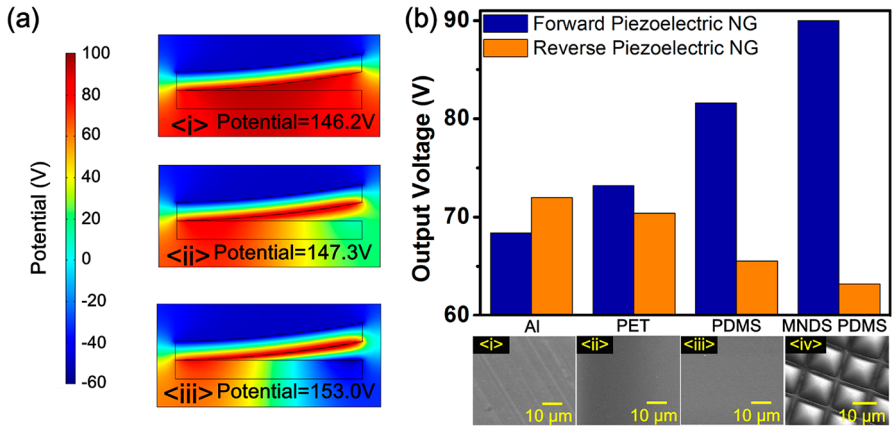

Figure 4. (a) Simulated piezoelectric output voltage with <i> 0 μC/m^2, <ii> 10 μC/m^2, and <iii> 20 μC/m^2 surface charge density. (b) Tested piezoelectric output voltage with <i> Al, <ii> PET, <iii> PDMS, <iv> MNDS PDMS substrate. The blue column indicates piezoelectric NG with forward polarity. The orange column indicates piezoelectric NG with reversed polarity. SEM images of the four different substrates are shown below the histogram.

piezoelectric NG, while the value of the triboelectric NG is 0.82 mW/cm^2. Compared with previous piezoelectric NGs[31] and triboelectric NGs,[18] the values are increased by 2.82 and 1.55 times, respectively. Besides the instantaneous power density, charging ability of the hybrid NG is also measured and analyzed. In the experiment, a 5 Hz external force is applied to the hybrid NG. The generated voltage is then rectified to continuously charge a 1 μF capacitor. For the piezoelectric NG, the voltage reaches 16.6 V in 120 s (Figure 3e), while a voltage of 13.0 V is achieved for the triboelectric NG (Figure 3f). It should be mentioned that the different charging ability of the two NGs is determined by the amplitude and duration of the output voltage. For the piezoelectric NG, although the amplitude of the voltage is relatively low, longer duration makes the charging ability better than that of the triboelectric NG.

Enhanced Piezoelectricity. Through combination of the piezoelectric NG and the triboelectric NG, the piezoelectricity can be enhanced due to the electric charges generated by friction.[32] To verify this, finite element method (FEM) simulation is conducted using the COMSOL software package. In the simulation, PVDF is placed on a PDMS substrate. The lower surface of PVDF and the upper surface of PDMS are charged with the same surface density but opposite polarity (positive charge in PVDF, negative charge in PDMS). As shown in Figure 4a, PVDF is bent to produce piezoelectric potential. Meanwhile, charges in the interface produce an electrostatic field, which will affect the original piezoelectric potential. In Figure 4a<i>, the surface charge density is zero and the piezoelectric potential is 146.2 V. With the increased surface charge density, the potential can be enhanced. In Figure 4a<ii>, the surface charge density is 10 μC/m^2 and the potential is increased to 147.3 V. When the surface charge density is doubled (*i.e.*, 20 μC/m^2), the potential is further enhanced to 153.0 V, as shown in Figure 4a<iii>.

The enhancement of piezoelectricity is also proved by experimental measurement. First, the influence of substrate material is investigated by placing PVDF onto three different substrates (*i.e.*, Al, PET, and PDMS). According to the triboelectric series,[33] the friction between the bottom Al electrode and the PDMS substrate will produce most triboelectric charges. As for the Al substrate, triboelectric charges are minimized. Due to the influence of triboelectric charges, the output voltage of piezoelectric NGs is enhanced. As shown in Figure 4b (blue column), when the substrate is changed from Al to PDMS, the peak–peak voltage of a forward piezoelectric NG is enhanced from 68.4 V (Al substrate) to 81.6 V (PDMS substrate). In addition, by using the micro/nanostructured PDMS substrate, the surface roughness is increased dramatically and more triboelectric charges can be generated in the micro/nanostructured surfaces,[20,27] thus further enhancing the piezoelectric output to 90.0 V. It is worth mentioning that the right polarity of the piezoelectric NG is essential for the enhancement. When the polarity is reversed, triboelectric charges will lead to the decline of peak–peak voltage. As indicated in the orange column in Figure 4b, the peak–peak voltage is reduced from 72.0 to 63.2 V by changing the substrate from Al to micro/nanostructured PDMS. Detailed time domain output voltage is shown in Figure S4 in the Supporting Information.

The enhanced or reduced piezoelectric output consists of two parts. The first part is the original piezoelectric output. The second part is the accumulated triboelectric charges, which contributes to the enhancement or reduction. In the enhancing case, positive triboelectric charges will accumulate on the bottom Al electrode and flow to the top Al electrode where the electric potential is lower. The flow of these charges will produce an additional potential difference in the external load. Therefore, the total piezoelectric output voltage is enhanced, which is the sum of the first and second part. If the polarity of PVDF is reversed,

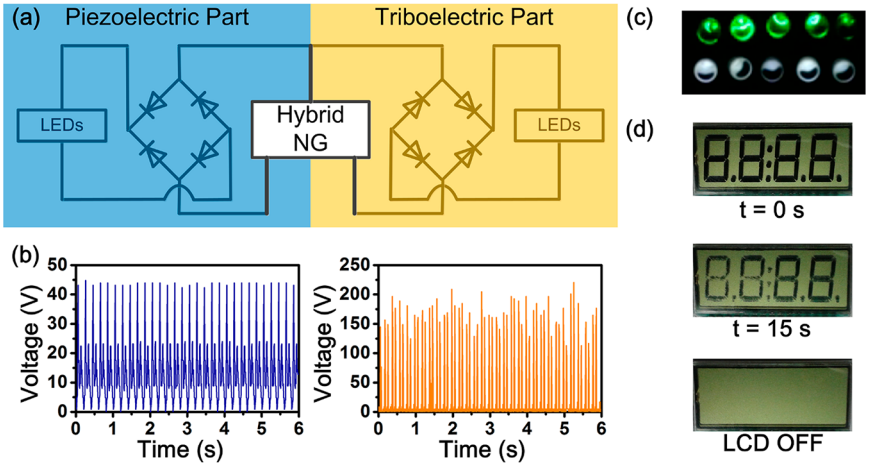

Figure 5. (a) Circuit diagram of the hybrid NG for lighting LEDs. (b) Rectified output voltage of the piezoelectric NG (left) and triboelectric NG (right). (c) LEDs lit by the hybrid NG. (d) Four-bit LCD displayed continuously by one cycle electric generation of the hybrid NG at t = 0 s (top) and t = 15 s (middle). The bottom image shows the off sate of the LCD.

the triboelectric charges will exist at the low electric potential electrode. This will to some extent prevent the original piezoelectric current flow, which will cause the reduced piezoelectric output.

Applications. For practical applications, the hybrid NG should have a large and stable output. Therefore, reliability of the hybrid NG is tested as shown in Figure S5 in the Supporting Information. With a 10 Hz external force, both the piezoelectric NG and triboelectric NG work very well continuously for 6000 cycles. With a stable and large enough output, capacitors can be charged to power microelectronic devices. To demonstrate, output voltage of the hybrid NG is first rectified to instantaneously light up commercial light-emitting diodes (LEDs). The hybrid NG is a three-terminal device (Figure 5a), as the bottom Al electrode is shared by the piezoelectric NG and triboelectric NG. Figure 5b shows the rectified output voltage of the piezoelectric and triboelectric NG. With a gentle finger typing, 10 LEDs are lighted up. The green LEDs are lighted by the piezoelectric NG, while the white LEDs are lighted by the triboelectric NG (Figure 5c). More details are shown in video 1 in the Supporting Information. In addition, the high output capability of the hybrid NG is verified by lighting a 4-bit liquid crystal display (LCD) screen. Through one cycle of electric generation, the LCD screen can be lighted continuously for tens of seconds. As shown in Figure 5d, after 15 s, all the numbers can still be clearly observed. Video 2 in the Supporting Information shows the detailed changes of the LCD screen.

This r-shaped hybrid NG can be easily integrated thanks to the flat and selectable friction substrate. For instance, the hybrid NG can be integrated inside a keyboard, in which case the plastic film of the keyboard works as the friction substrate. In the typing process, the hybrid NG is pressed and released thus producing electricity in daily use. Here, we put the hybrid NG under the space button of a keyboard. With normal typing, peak voltage of about 20 V is obtained, as is demonstrated in video 3 in the Supporting Information.

CONCLUSION

In this work, an r-shaped hybrid NG is developed and investigated. By using PVDF, nanostructured Al and MNDS PDMS, we innovatively combine the piezoelectric NG and the triboelectric NG together to enhance the output performance. With a 5 Hz periodic external force, the output peak voltage, the current density, and the volume power density of the piezoelectric NG reach 52.8 V, 20.75 μA/cm^2, and 10.95 mW/cm^3, respectively. For the triboelectric NG, the values are 240 V, 3.40 μA/cm^2, and 2.04 mW/cm^3, respectively. Through triboelectrification, the piezoelectric output can be enhanced. With different friction materials and piezoelectric polarities, output peak–peak voltage of the piezoelectric NG varies from 63.2 to 90.0 V. This is a new approach to enhance the output of piezoelectric NGs, which is simple, low-cost, and effective. The large output enables this hybrid NG to power personal electronics with LEDs and LCDs, which shows attractive potential applications for self-powered systems. In addition, because of the specially designed r-shaped structure, the hybrid NG can be easily integrated to other devices, which makes it possible to harvest energy from daily life.

EXPERIMENTAL SECTION

Fabrication of Micro/Nanostructured Silicon Mold and PDMS. First, a 1000 Å Si_3N_4 layer is deposited and patterned by photolithography and reactive ion etching (RIE). Then, KOH wet etching is conducted at 85 °C to form the microstructures. After removing the Si_3N_4 layer, nanostructures are fabricated through an improved deep reactive ion etching (DRIE) process. The micro/nanostructured PDMS is fabricated by replicating from the

silicon mold. First, the base solution and the curing agent of commercial PDMS (Sylgard 184, Dow Corning Corporation) are mixed with a quantity ratio of 10:1. The mixture is then poured onto the prefabricated micro/nanostructured silicon mold. Afterward, the vacuumization process is conducted to remove the air bladder at the interface, which is beneficial to form well-shaped micro/nanostructures. Finally, the micro/nanostructured PDMS is peeled off after heating at 80 °C for 30 min. Detailed fabrication flowchart is shown in Figure S6 in the Supporting Information.

Fabrication of Surface-Nanostructured Al Electrode. The Al electrode is first evaporated onto the PVDF thin film and then immersed into hot deionized water at 70 °C. After 15 min reaction, the surface of Al electrode is covered with nanostructures, whose average size is approximately 200 nm.

Measurement System. In the measurement process, the top of the device is fixed to a certain place and the bottom part is placed onto a vibration plate to obtain a periodic external force. The excitation signal is a sinusoidal wave with 1 V amplitude, produced by a waveform generator (RIGOL DG1022). The signal is then amplified by an amplifier (SINOCERA YE5871A) to drive the vibration plate (SINOCERA). For output characterization, the external force frequency is set at 5 Hz, while 10 Hz external force is applied in the reliability test. All the signals are recorded and displayed through a digital oscilloscope (RIGOL DS1102E).

Conflict of Interest: The authors declare no competing financial interest.

Acknowledgment. This work is supported by the National Natural Science Foundation of China (Grant Nos. 91023045 and 61176103), Development Program ("863" Program) of China (Grant No. 2013AA041102), National Ph.D. Foundation Project (20110001110103), and Key Laboratory Fund (No. 9140C790103110C7903).

Supporting Information Available: (1) Triboelectric output with different morphologies; (2) equivalent resistance model for the triboelectric NG; (3) overall output of the hybrid NG; (4) time domain piezoelectric output voltage with different substrates; (5) reliability test of the hybrid NG; (6) fabrication process of the micro/nano dual-scale PDMS; (7) supplementary videos of LEDs lighted instantaneously by the hybrid NG, LCD displaying continuously by one cycle electric generation, and electricity generated by pressing a keyboard. This material is available free of charge *via* the Internet at http://pubs.acs.org.

REFERENCES AND NOTES

1. Lewis, N. S. Toward Cost-Effective Solar Energy Use. *Science* **2007**, *315*, 798–801.
2. Roy, S. C.; Varghese, O. K.; Paulose, M.; Grimes, C. A. Toward Solar Fuels Photocatalytic Conversion of Carbon Dioxide to Hydrocarbons. *ACS Nano* **2010**, *4*, 1259–1278.
3. Wang, X.; Song, J.; Liu, J.; Wang, Z. L. Direct-Current Nanogenerator Driven by Ultrasonic Waves. *Science* **2007**, *316*, 102–105.
4. Beeby, S. P.; Tudor, M. J.; White, N. M. Energy Harvesting Vibration Sources for Microsystems Applications. *Meas. Sci. Technol.* **2006**, *17*, R175–R195.
5. Beeby, S. P.; Torah, R. N.; Tudor, M. J.; Glynne-Jones, P.; O'Donnell, T.; Saha, C. R.; Roy, S. A Micro Electromagnetic Generator for Vibration Energy Harvesting. *J. Micromech. Microeng.* **2007**, *17*, 1257–1265.
6. Basset, P.; Galayko, D.; Mahmood Paracha, A.; Marty, F.; Dudka, A.; Bourouina1, T. A Batch-Fabricated and Electret-Free Silicon Electrostatic Vibration Energy Harvester. *J. Micromech. Microeng.* **2009**, *19*, 115025-1–115025-12.
7. Elfrink, R.; Kamel, T. M.; Goedbloed, M.; Matova, S.; Hohlfeld, D.; van Andel, Y.; van Schaijk, R. Vibration Energy Harvesting with Aluminum Nitride-Based Piezoelectric Devices. *J. Micromech. Microeng.* **2009**, *19*, 094005-1–094005-8.
8. Wang, Z. L.; Song, J. Piezoelectric Nanogenerators Based on Zinc Oxide Nanowire Arrays. *Science* **2006**, *312*, 242–246.
9. Chang, C.; Tran, V. H.; Wang, J.; Fuh, Y.-K.; Lin, L. W. Direct-Write Piezoelectric Polymeric Nanogenerator with High Energy Conversion Efficiency. *Nano Lett.* **2010**, *10*, 726–731.
10. Chen, X.; Xu, S.; Yao, N.; Shi, Y. 1.6 V Nanogenerator for Mechanical Energy Harvesting Using PZT Nanofibers. *Nano Lett.* **2010**, *10*, 2133–2137.
11. Park, K.-I.; Lee, M.; Liu, Y.; Moon, S.; Hwang, G.-T.; Zhu, G.; Kim, J. E.; Kim, S. O.; Kim, D. K.; Wang, Z. L.; *et al.* Flexible Nanocomposite Generator Made of $BaTiO_3$ Nanoparticles and Graphitic Carbons. *Adv. Mater.* **2012**, *24*, 2999–3004.
12. Lee, T. I.; Lee, S.; Lee, E.; Sohn, S.; Lee, Y.; Lee, S.; Moon, G.; Kim, D.; Kim, Y. S.; Myoung, J. M.; *et al.* High-Power Density Piezoelectric Energy Harvesting Using Radially Strained Ultrathin Trigonal Tellurium Nanowire Assembly. *Adv. Mater.* **2013**, *25*, 2920–2925.
13. Xu, S.; Yeh, Y.-w.; Poirier, G.; McAlpine, M. C.; Register, R. A.; Yao, N. Flexible Piezoelectric PMN-PT Nanowire-Based Nanocomposite and Device. *Nano Lett.* **2013**, *13*, 2393–2398.
14. Fan, F.-R.; Tian, Z.-Q.; Wang, Z. L. Flexible Triboelectric Generator!. *Nano Energy* **2012**, *1*, 328–334.
15. McCarty, L. S.; Whitesides, G. M. Electrostatic Charging Due to Separation of Ions at Interfaces Contact Electrification of Ionic Electrets. *Angew. Chem., Int. Ed.* **2008**, *47*, 2188–2207.
16. Wang, S.; Lin, L.; Wang, Z. L. Nanoscale Triboelectric-Effect-Enabled Energy Conversion for Sustainably Powering Portable Electronics. *Nano Lett.* **2012**, *12*, 6339–6346.
17. Tang, W.; Meng, B.; Zhang, H. X. Investigation of Power Generation Based on Stacked Triboelectric Nanogenerator. *Nano Energy* **2013**, 10.1016/j.nanoen.2013.04.009.
18. Wang, S.; Lin, L.; Xie, Y.; Jing, Q.; Niu, S.; Wang, Z. L. Sliding-Triboelectric Nanogenerators Based on In-Plane Charge-Separation Mechanism. *Nano Lett.* **2013**, *13*, 2226–2233.
19. Zhu, G.; Chen, J.; Liu, Y.; Bai, P.; Zhou, Y. S.; Jing, Q.; Pan, C.; Wang, Z. L. Linear-Grating Triboelectric Generator Based on Sliding Electrification. *Nano Lett.* **2013**, *13*, 2282–2289.
20. Zhang, X. S.; Han, M. D.; Wang, R. X.; Zhu, F. Y.; Li, Z. H.; Wang, W.; Zhang, H. X. Frequency-Multiplication High-Output Triboelectric Nanogenerator for Sustainably Powering Bio-Medical Microsystems. *Nano Lett.* **2013**, *13*, 1168–1172.
21. Lin, Z.-H.; Zhu, G.; Zhou, Y. S.; Yang, Y.; Bai, P.; Chen, J.; Wang, Z. L. A Self-Powered Triboelectric Nanosensor for Mercury Ion Detection. *Angew. Chem.* **2013**, *125*, 5169–5173.
22. Lin, Z.-H.; Xie, Y.; Yang, Y.; Wang, S.; Zhu, G.; Wang, Z. L. Enhanced Triboelectric Nanogenerators and Triboelectric Nanosensor Using Chemically Modified TiO_2 Nanomaterials. *ACS Nano* **2013**, *7*, 4554–4560.
23. Yang, Y.; Zhang, H.; Liu, Y.; Lin, Z.-H.; Lee, S.; Lin, Z.; Wong, C. P.; Wang, Z. L. Silicon-Based Hybrid Energy Cell for Self-Powered Electrodegradation and Personal Electronics. *ACS Nano* **2013**, *7*, 2808–2813.
24. Yang, Y.; Zhang, H.; Chen, J.; Lee, S.; Hou, T.-C.; Wang, Z. L. Simultaneously Harvesting Mechanical and Chemical Energies by a Hybrid Cell for Self-Powered Biosensors and Personal Electronics. *Energy Environ. Sci.* **2013**, *6*, 1744–1749.
25. Peter, N. J.; Zhang, X. S.; Chu, S. G.; Zhu, F. Y.; Zhang, H. X. Tunable Wetting Behavior of Nanostructured Poly-(dimethylsiloxane) by Plasma Combination Treatments. *Appl. Phys. Lett.* **2012**, *101*, 221601-1–221601-4.
26. Cortese, B.; D'Amone, S.; Manca, M.; Viola, I.; Cingolani, R.; Gigli, G. Superhydrophobicity Due to the Hierarchical Scale Roughness of PDMS Surfaces. *Langmuir* **2008**, *24*, 2712–2718.
27. Fan, F.-R.; Lin, L.; Zhu, G.; Wu, W.; Zhang, R.; Wang, Z. L. Transparent Triboelectric Nanogenerators and Self-Powered Pressure Sensors Based on Micropatterned Plastic Films. *Nano Lett.* **2012**, *12*, 3109–3114.
28. He, M.; Zhang, Q.; Zeng, X.; Cui, D.; Chen, J.; Li, H.; Wang, J.; Song, Y. Hierarchical Porous Surface for Efficiently Controlling Microdroplets Self-Removal. *Adv. Mater.* **2013**, *25*, 2291–2295.

29. Castle, G. S. P. Contact Charging between Insulators. *J. Electrost.* **1997**, *40*, 13–20.
30. Lu, F.; Lee, H. P.; Lim, S. P. Modeling and Analysis of Micro Piezoelectric Power Generators for Micro-Electromechanical-Systems Applications. *Smart Mater. Struct.* **2004**, *13*, 57–63.
31. Saravanakumar, B.; Mohan, R.; Thiyagarajan, K.; Kim, S.-J. Fabrication of ZnO Nanogenerator for Eco-Friendly Bio-mechanical Energy Harvesting. *RSC Adv.* **2013**, *3*, 16646–16656.
32. Kim, H.; Kim, S. M.; Son, H.; Kim, H.; Park, B.; Ku, J. Y.; Sohn, J. I.; Im, K.; Jang, J. E.; Park, J.-J.; *et al.* Enhancement of Piezoelectricity *via* Electrostatic Effects on a Textile Platform. *Energy Environ. Sci.* **2012**, *5*, 8932–8936.
33. Diaz, A. F.; Felix-Navarro, R. M. A Semi-quantitative Tribo-electric Series for Polymeric Materials: The Influence of Chemical Structure and Properties. *J. Electrost.* **2004**, *62*, 277–290.